Journal of Visualized Experiments

Formulation and Acoustic Modulation of Optically Vaporized Perfluorocarbon Nanodroplets

--Manuscript Draft--

Article Type:	Invited Methods Collection - JoVE Produced Video
Manuscript Number:	JoVE62814R1
Full Title:	Formulation and Acoustic Modulation of Optically Vaporized Perfluorocarbon Nanodroplets
Corresponding Author:	Stanislav Emelianov UNITED STATES
Corresponding Author's Institution:	
Corresponding Author E-Mail:	stas@gatech.edu;emelian@mail.utexas.edu
Order of Authors:	Andrew Zhao
	Jeungyoon Lee
	Stanislav Emelianov
Additional Information:	
Question	**Response**
Please specify the section of the submitted manuscript.	Bioengineering
Please indicate whether this article will be Standard Access or Open Access.	Standard Access ($1400)
Please indicate the **city, state/province, and country** where this article will be **filmed**. Please do not use abbreviations.	Atlanta, GA, USA
Please confirm that you have read and agree to the terms and conditions of the author license agreement that applies below:	I agree to the Author License Agreement
Please provide any comments to the journal here.	
Please confirm that you have read and agree to the terms and conditions of the video release that applies below:	I agree to the Video Release

JOURNAL OF VISUALIZED EXPERIMENTS
1 Alewife Center #200
Cambridge, MA 02140
tel. 617.945.9051
www.jove.com

Standard Manuscript Template

TITLE:

Formulation and Acoustic Modulation of Optically Vaporized Perfluorocarbon Nanodroplets

AUTHORS AND AFFILIATIONS:

Andrew Zhao[1], Jeungyoon Lee[2], Stanislav Emelianov[1,3]

[1]Department of Biomedical Engineering at Georgia Institute of Technology and Emory University
[2]School of Electrical Engineering at Georgia Institute of Technology

[3]Department of Biomedical Engineering at Georgia Institute of Technology and Emory University and School of Electrical Engineering at Georgia Institute of Technology

Corresponding Author:
Stanislav Emelianov (stas@gatech.edu)

Email Addresses of Co-Authors:
Andrew Zhao (azhao36@gatech.edu)
Jeungyoon Lee (jyoon.lee@gatech.edu)
Stanislav Emelianov (stas@gatech.edu)

KEYWORDS:

ultrasound, perfluorocarbon nanodroplets, nanodroplets, contrast agents, emulsion, nanoparticle, photoacoustic, phase-change,

SUMMARY:

Optically activated perfluorocarbon nanodroplets show promise in imaging applications outside of the vascular system. This article will demonstrate how to synthesize these particles, crosslink polyacrylamide phantoms, and modulate the droplets acoustically to enhance their signal.

ABSTRACT:

Microbubbles are the most commonly used imaging contrast agent in ultrasound. However, due to their size, they are limited to vascular compartments. These microbubbles can be condensed or formulated as perfluorocarbon nanodroplets (PFCnDs) that are small enough to extravasate and then be triggered acoustically at the target site. These nanoparticles can be further enhanced by including an optical absorber such as near infrared organic dye or nanoparticles (e.g., copper sulfide nanoparticles or gold nanoparticles/nanorods). Optically tagged PFCnDs can be vaporized through laser irradiation in a process known as optical droplet vaporization (ODV). This process of activation enables the use of high boiling point perfluorocarbon cores, which cannot be vaporized acoustically under the maximum mechanical index threshold for diagnostic imaging. Higher boiling point cores result in droplets that will recondense after vaporization, resulting in "blinking" PFCnDs that briefly produce contrast after vaporization before condensing back into nanodroplet form. This process can be repeated to produce contrast on demand, allowing for the background free imaging, multiplexing, super-resolution, and contrast enhancement through

both optical and acoustic modulation. This article will demonstrate how to synthesize optically-triggerable, lipid shell PFCnDs utilizing probe sonication, create polyacrylamide phantoms to characterize the nanodroplets, and acoustically modulate the PFCnDs after ODV to improve contrast.

INTRODUCTION:

Microbubbles are the most ubiquitous ultrasound contrast agent owing to their biocompatibility and excellent echogenicity in comparison to soft tissues. This makes them valuable tools for visualizing blood flow, organ delineation, and other applications[1]. However, their size (1-10 µm), which makes them exceptional for imaging based on their resonant frequency, restricts their applications to the vasculature[2].

This limitation has led to the development of PFCnDs, which are nano-emulsions composed of a surfactant encased around a liquid perfluorocarbon core. These nanoparticles can be synthesized at sizes as small as 200 nm and are designed to take advantage of "leaky" vasculature or pores and open fenestrations found in tumor vasculature. While these disruptions are tumor dependent, this permeability allows for extravasation of nanoparticles from ~200 nm - 1.2 µm depending on the tumor[3,4]. In their initial form, these particles produce little to no ultrasound contrast. Upon vaporization – induced acoustically or optically – the core phase changes from liquid to gas, inducing a two and half to five-fold increase in diameter[5–7] and generating photoacoustic and ultrasound contrast. While acoustic vaporization is the most common activation method, this approach creates acoustic artifacts that limits the imaging of the vaporization. Additionally, most perfluorocarbons require focused ultrasound with a mechanical index beyond the safety threshold to vaporize[8]. This has led to the development of lower boiling point PFCnDs, which can be synthesized by condensing microbubbles into nanodroplets[9]. However, these droplets are more volatile and subject to spontaneous vaporization[10].

Optical droplet vaporization (ODV), on the other hand, requires the addition of an optical trigger such as nanoparticles[11–13] or dye[6, 14, 15] and can vaporize higher boiling point perfluorocarbons using fluences within the ANSI safety limit[11]. PFCnDs synthesized with higher boiling point cores are more stable and will recondense after vaporization, allowing for background free imaging[16], multiplexing[17], and super-resolution[18]. One of the major limitations of these techniques is the fact that high boiling point PFCnDs are echogenic after vaporization for only a short timeframe, on the scale of milliseconds[19], and are relatively faint. While this issue can be mitigated through repeated vaporizations and averaging, detection and separation of droplet signal remains a challenge.

Taking inspiration from pulse inversion, the duration and contrast can be enhanced by modifying the phase of the ultrasound imaging pulse[19]. By starting the ultrasound imaging pulse with a rarefaction phase (n-pulse), both the duration and contrast of the vaporized PFCnDs increases. In contrast, starting the ultrasound imaging pulse with a compression phase (p-pulse), results in reduced contrast and shorter in duration. This article will describe how to synthesize optically triggerable perfluorocarbon nanodroplets, polyacrylamide phantoms commonly used in imaging, and demonstrate contrast enhancement and improved signal longevity through acoustic

modulation.

PROTOCOL:

1. Perfluorocarbon nanodroplet formulation

1.1. Rinse out a 10 mL round-bottom flask with chloroform and wash out a 10 µL and 1 mL gas tight glass syringe with chloroform by repeatedly aspirating the full syringe volume and expelling it for a total of three times.

CAUTION: Chloroform is volatile and can be toxic if inhaled. All work with this solvent should be performed in a fume hood.

1.2. Using the syringes, add 200 µL of DSPE-mPEG2000 (25 mg/mL), 8 µL of 1,2-distearoyl-sn-glycero-3-phosphocholine (DSPC, 10 mg/mL) and 1 mL of IR 1048 (1 mg/mL in chloroform) into the round-bottom flask. Remember to clean out the syringes between lipids/dye to prevent contamination of the stock.

NOTE: Infrared dyes are light sensitive, and work should be done in dim conditions or flasks should be covered in aluminum foil.

1.3. Remove the solvent utilizing a rotary evaporator. Ensure that the vacuum is slowly adjusted to 332 mbar to prevent bumping. After 5 min, reduce the pressure to 42 mbar to remove any water that may have entered the solution.

NOTE: The lipid cake can be stored overnight in a round bottom flask covered with parafilm at 4 °C.

1.4. Suspend the lipid cake in 1 mL of phosphate buffered saline (PBS) and sonicate or vortex at room temperature for 5 min or until all of the lipid cake has been suspended and dissolved in the solution. Sonicate for an additional 2 min to homogenize the solution.

1.5. Transfer the solution to a 7 mL glass vial and place the vial in a glass dish filled with ice to allow the solution to cool down for 5 min before adding 50 µL of perfluorohexane using a gas tight glass syringe. Remember to rinse out the syringe with perfluorohexane before dispensing it into the vial.

1.6. Place the glass vial containing the lipids and ice bath in the probe sonicator enclosure and submerge the probe tip below the miniscus. Ensure that the sides of the sonicator probe does not touch the lip of the glass vial.

1.7. Probe sonicate the mixture with the following settings: Amplitude 1, Process time: 20 s, Pulse-On: 1s, Pulse-off: 5s. Then sonicate at the following settings: Amplitude: 50, Process time: 5 s, Pulse-on: 1 s, Pulse-off: 10 s.

1.8. Transfer the nanodroplet solution to a 1.5 mL centrifuge tube and centrifuge at 300 x *g* for 3 min to separate out the larger droplets (>1 µm) from smaller droplets.

1.9. Discard the pellet and transfer the supernatant to another 1.5 mL centrifuge tube. Wash the supernatant by centrifuging at 3000 x *g* for 5 min to pellet all the droplets in solution. Resuspend the PFCnDs in 1 mL of PBS by pipetting the pellet up and down and then sonicate in a bath sonicator for 1 min.

1.10. Measure the size of the droplets using dynamic light scattering (DLS). Dilute the stock PFCnDs by 100-fold (10 µL of PFCnD stock in 990 µL of PBS) and bath sonicate to disperse the PFCnDs before measuring. Representative results are shown in **Figure 1**.

1.11. Determine the concentration of the PFCnDs utilizing the nanoparticle tracking analyzer (see **Table of Materials**). Dilute the PFCnDs by 100-1000-fold to ensure accurate measurement of the concentration. The protocol typically yields droplets at a concentration on the order of 10^{10} particles/mL.

1.12. Prepare 10 mL of ultrasound coupling gel in a 50 mL centrifuge tube and add 1% (v/v) or 100 µL of PFCnDs to make solution of ~10^8 particles/mL. Vortex the solution to mix. Centrifuge the mixture at 4000 x *g* for 3 min to remove bubbles.

2. Polyacrylamide phantom preparation

2.1. Degas water by filling a 500 mL vacuum flask with 400 mL of deionized water, seal with a rubber cork, and connect the flask to the vacuum line. Open the vacuum line and submerge the bottom of the flask in the bath sonicator. Sonicate for 5 min or until no gas bubble formation is visible.

2.2. Prepare 10% ammonium persulfate (APS) solution by dissolving 500 mg in 5 mL of degassed water. Gently swirl the solution if the ammonium persulfate does not fully dissolve.

2.3. In a 400 mL beaker with a stir bar on a stir plate, add 150 mL of degassed water and 50 mL of 40% (w/v) acrylamide-bisacrylamide solution to form 200 mL of 10% acrylamide-bisacrylamide solution. Stir the mixture at 200 rpm to allow for the proper mixing without introducing bubbles.

CAUTION: Acrylamide is a carcinogen, and all work should be done in a fume hood with gloves, especially if working with acrylamide in powder form.

2.4. Weigh out 400 mg of silica to and add it to the 10% acrylamide-bisacrylamide solution from step 2.3 to form a 0.2 %(w/v) of silica and acrylamide solution.

CAUTION: Silica when inhaled can be a carcinogen. All work including weighing should be

performed in a fume hood.

2.5. Prepare a 58 mm x 58 mm x 78 mm square mold with a cylindrical inclusion by cutting off the tips of from a plastic transfer pipette and supporting it in the mold with lab tape. See **Figure 2**.

2.6. Add 2 mL of 10 % APS solution to the beaker to make a final concentration of 0.1% APS and add 250 µL of Tetramethylethylenediamine (TEMED) to the phantom solution. Allow the solution to stir briefly (less than a min).

2.7. Quickly pour the solution into the mold, while being careful not to introduce air bubbles into the solution. The solution should polymerize within 10 min. Remove the phantom by running the flat end of a lab spatula around the edge of the mold and inverting the mold.

NOTE: These phantoms can be reused multiple times and should be submerged in water and stored at 4°C.

3. Perfluorocarbon nanodroplet imaging

3.1. Turn on and warm up the pulsed laser system for ~20 min following manufacturer instructions. Ensure that the fiber optical bundle is properly connected to the laser output and the two legs are properly placed within the fiber bundle holder.

3.2. Turn on the ultrasound imaging system, connect array imaging transducer (L11-4v) to the system and fix the transducer within the holder to align its imaging plane with laser cross section.

3.3. Set the pulse repetition frequency of the laser system to 10Hz and place a powermeter at the end of the fiber bundle to measure energy. Tune the q-switch delay until the estimated fluence is 70 mJ/cm^2.

CAUTION: Appropriate eyewear must be worn when firing the laser and laser curtains must enclose the space.

3.4. Backfill one of the channels in the polyacrylamide phantom with the ultrasound gel/PFCnD mixture using a 1 mL plastic slip tip syringe. Liberally cover the top of the channel with ultrasound gel and remove any bubbles with a 1 mL plastic slip tip syringe. Place the polyacrylamide phantom underneath the transducer and fiber bundle as shown in **Figure 3**.

3.5. Use the combined laser ultrasound and elasticity (CLUE) imaging platform based on the software[20] to image PFCnD synchronized with optical activation. Change the general user-defined parameters in **Param** structure for imaging: set start/end depth to 0/40mm, center frequency to 6.9MHz, and transducer name to 'L11-4v'.

3.6. Define a new **RunCase** and design a module sequence for repeated optical

activation/recondensation and US imaging of PFHnDs. This is done by listing predefined modules such as ultrafast imaging (mUF), external laser (mExtLaser) and idle(mIdle).

3.6.1. Repeat the sequence set **mExtLaser-mIdle-mUF-mExtLaser-mUF** twice to acquire both n-pulse and p-pulse imaging data.

NOTE: The first **mExtLaser** module in each sequence is set as a sham laser by setting **ExtLaser.Enable** to 0 and the 'mIdle' is included to minimize time between background US images and the n/p-pulse US images after laser activation.

3.7. Set module parameters for each module placed in the current run case's module sequence. Access each module parameter by index corresponding to its order in module sequence. Modules will execute pre-defined operations with module parameters user set here.

3.7.1. Set **ExtLaser.QSdelay** in external laser modules to the value of laser Q-switch delay tuned in step 3.3, in microseconds. This module waits for laser system's flashlamp trigger out and generates Q-switch trigger after the delay specified in **QSdelay**.

3.7.2. In ultrafast imaging module, set **Resource.numFrame** to 100, set **SeqControl.PRI** to 200 (µs), and set **TW.polarity** to 1 for P-pulse and -1 for N-pulse (see **Figure 4** for corresponding pulse shape). This module will transmit ultrafast 0-degree planar wave with pulse type specified in **TW.polarity**.

3.7.2.1. Acquire full aperture imaging window of 38.8 mm wide for number of frames in **Resource.numFrame**, pulse repetition interval of **SeqControl.PRI**, then save data for off-line processing.

3.7.3. Set **SeqControl.lastPRI_Module** in idle module to the length of time between laser pulses (100 ms) subtracted by Q-switch delay, imaging data acquisition time (20 ms), and a 20 µs margin for the signal to travel. This module keeps the system under 'no operation' state for the time in **SeqControl.lastPRI_Module** to fill the time gap between the end of imaging data acquisition and next laser pulse excitation.

REPRESENTATIVE RESULTS:

Successful formulation and centrifugal separation of the PFCnDs should yield droplets around the size of 200-300 nm in diameter (**Figure 1A**). Improperly separated droplets may show small peaks around 1 µm. These solutions can be further bath sonicated to break up the larger droplets. The size of the droplets will increase over time due to coalescing and/or diffusion in a process known as Ostwald ripening[21,22] (**Figure 1B**).

Acoustic modulation of the droplets by manipulating the imaging pulse improved the contrast of the vaporized PFCnDs. This was demonstrated in PFCnD images reconstructed by subtracting adjacent frames of the beamformed images so that only the signal returned from vaporized PFCnD is visible and stationary background signal is suppressed. Contrast is quantified by the

ratio of the difference between average signals of the circular inclusion area and average background signal over average background signal. The background signal is defined by the signals from two rectangular ROIs of the background that are at the same depth and equivalent area as the inclusions. The contrast from the inclusion for the N-pulse is approximately 3.2 times greater (*i.e.*, 220 % improvement) than the P-pulse (**Figure 5**).

The inversed imaging pulse also increased the longevity of the signal from PFCnD vaporization. This was quantified by thresholding the pixels in the circular inclusion region that exceeds the background signal. The percentage of pixels in the inclusion that was above the threshold was defined as the hyperechoic area (%). To examine the PFCnDs' hyperechogenic behavior over time, hyperechoic area is calculated for each frame and normalized by the hyperechoic area of the first frame, and then fitted to an exponential decay model. This function was used to determine the characteristic decay time, defined as the timespan it takes for the hyperechoic area after PFCnD activation to decay to only 10 % of the initial area (**Figure 6a**). The characteristic decay time of normalized hyperechoic area is up to 3.5 times longer in N-pulse imaging compared to P-pulse. Representative B-mode differential image frames in time for each N-pulse and P-pulse imaging are shown in **Figure 6b**.

FIGURE AND TABLE LEGENDS:

Figure 1: DLS size measurements of PFCnDs and stability. (**A**) The size intensity distribution of droplets averaged from three measurements of droplets after synthesis (average PDI: 0.132± 0.016; average Z-average: 259.3 ± 0.7 nm). (**B**) The size intensity distribution of droplets averaged from three measurements taken 24 hours after synthesis (average PDI: 0.252± 0.061; average Z-average: 322.5 ± 4.5 nm).

Figure 2: Image and schematic of polyacrylamide mold. (**A**) Image of the mold made from lab tape and the plastic container. (**B**) Schematic with measurements of the polyacrylamide phantom after removal from mold.

Figure 3: A schematic of the laser pulse delivery and ultrasound imaging. (**A**) Components of the assembly are labeled and laser beam / ultrasound imaging plane alignment relative to the inclusion position is illustrated. (**B**) An image showing the actual setup.

Figure 4: Simulated ultrasound imaging pulse. The waveforms are simulated by ultrasound imaging system software, sampled by 250 MHz. The waveform of P-pulse and N-pulse are generated with the same center frequency and pulse width but have 180˚ of phase difference.

Figure 5: Contrast measurement. Mean contrast value of inclusion area for N-pulse and P-pulse, error bars represent standard deviation (n=3).

Figure 6: Characteristic decay curve of hyperechoic area and representative differential B-mode mages. (**A**) Normalized hyperechoic area induced by PFCnD activation over time for N-pulse and P-pulse imaging at the same cross-section. The dotted line indicates 10% of the initial

hyperechoic area. The time at which the fitted plot intersects with the dotted line represents the characteristic decay time. (**B**) Images show a cropped ROI window centered on the inclusion, plotted on a dB scale with a dynamic range of 35. The top row shows the recondensing behavior imaged by the P-pulse and the lower row shows the N-pulse. The yellow-colored dashed line indicates the inclusion area.

Table 1: Summary of the reagents and amounts for polyacrylamide phantom crosslinking based on mold volume. This table provides a concise value summary of the reagents used and amounts based upon several common mold volumes.

DISCUSSION:

Probe sonication is a relatively simple and easy to learn method to fabricate PFCnDs. There are a few steps where care must be taken. When handling chloroform, it is imperative that a positive displacement pipette or glass syringes is used, as it is volatile and will "leak" from standard air displacement pipettes. Furthermore, if using a positive displacement, ensure that an appropriate tip is used as chloroform will dissolve most plastic tips, which can introduce contaminants into the solution. A positive displacement pipette or glass syringe is also recommended for perfluorohexane, as it is both volatile and denser than water. Typically, the individual effects of volatility and high density can be reduced by pre-wetting in air displacement pipettes and using a scale to adjust the volume set on the pipette, respectively. But in the case of perfluorohexane which possesses both properties, the volatility will make it difficult to obtain accurate weight measurements, making a positive displacement pipette/glass syringe the most viable option.

Before probe sonicating the solution, it is important to incubate the lipid and perfluorocarbon solution in an ice bath to allow it to cool down to prevent boiling the perfluorocarbon during sonication. This step will be especially important for lower boiling perfluorocarbon such as perfluoropentane. Furthermore, care must be taken when probe sonicating the solution. The sonication probe tip should be submerged, but it should not make contact with the bottom or sides of the glass vial as it could damage the tip and shatter the vial, emptying the lipid solution into the ice bath.

The PFCnD fabrication protocol can be adapted in a few minor ways. If a rotary evaporator is unavailable in step 1.3, the solution can be dried with a steady stream of nitrogen gas or be placed in a vacuum chamber overnight to form the lipid cake. Regarding the lipids, this formulation utilizes a 9:1 ratio of DSPE-PEG:DSPC compared to the standard 1:9 ratio of DSPE-PEG:DSPC, because it results in smaller and more size stable droplets[23]. This formulation can be adapted to allow for surface conjugation by substituting a small fraction (~2 mol %) of the DSPE-PEG with a functionalized DSPE-PEG with the desired moiety (e.g., biotin, thiol, amine, etc.).

In general, probe sonicators are commercially available, relatively simple to use, and can be easily adapted to other higher boiling point perfluorocarbons and surfactant formulations, but it cannot be used to make droplets with perfluorocarbon cores that are gaseous at room temperature without significant modifications. One such modification is utilizing probe sonication to create microbubbles and then applying pressure and reducing the temperature to condense the

microbubbles into droplets[24]. While this method is a clever way to generate acoustically vaporizable droplets, it is difficult to encapsulate enough dye within the microbubbles to ensure ODV after condensation. An alternative approach is to conjugate the dye (e.g., Cy7.5) to the lipids and form microbubbles which can be condensed down into ODV capable low boiling point PFCnDs[25].

Probe sonication also produces a high concentration of nanodroplets (~10^{10} droplets/mL) in a relatively short period of time. However, this technique results in a large size distribution that will reduce the amount of nanodroplets that will extravasate. While, this can be ameliorated through centrifugal filtering or syringe filters to remove larger droplets, the resulting PFCnDs will exhibit greater polydispersity in comparison to droplets synthesized using microfluidics or filtered through extrusion[26]. Another drawback to probe sonication is that the sonication probe tip will inevitably become pitted from cavitation during sonication and will need to be replaced periodically.

An alternative approach to creating droplets utilizes microfluidic devices which can be used to tailor droplets to a specific size with a low polydispersity index (PDI). However, these devices produce droplets at a relatively slow rate (~10^4-10^6 droplets/s)[26] and, while there have been several developments such as step emulsification[27], tip streaming in flow focusing devices[28, 29], and utilizing the ouzo effect with a staggered herringbone micromixer[30] - generating nanosized droplets still remains challenging. Furthermore, this technique is not commercially available, and the fabrication of these devices requires specialized expertise.

Other methods that are commercially available include extrusion and homogenization. Extrusion utilizes membranes to pass droplets through, resulting in nano-sized droplets with a narrower size range compared to sonication. However this method is heavily formulation dependent and is challenging to incorporate dye or therapeutic cargo within the droplet[26]. High pressure homogenization makes use of commercially available homogenizers that utilize high pressure and shear stress to generate monodisperse, nanoscale lipid particles in a scalable fashion[31–33]. This method has been adapted to create droplets with high and low boiling point perfluorocarbons[32,34]. A more substantial review of droplet formulation methods and sample protocols can be found in the following review[26].

Phantoms are a valuable tool to characterize the performance of nanodroplets *in vitro*. In this protocol, polyacrylamide-based phantoms with silica are used. The most frequent issues with polyacrylamide phantoms are related to slow or no polymerization. Slow polymerization, while less problematic, can lead to heterogeneous distribution of embedded scatter. The most common culprit for this issue is the use of old solutions of ammonium persulfate that reduce the production of free radicals that initiate the crosslinking. This can be easily addressed by making the solution fresh or not using prepared solutions that are older than one week. Another possibility is the degradation of TEMED – this will be evident in the formation of a yellow precipitate. One other common issue is the presence of air bubbles in the polymerized phantom. Proper degassing of the water and careful handling to avoid excess surface agitation should mitigate this issue. An alternative strategy would be to degas the entire solution after step 2.5.

However, this should be performed in a fume hood due to the presence of acrylamide.

These phantoms are also excellent for imaging the behavior of restricted droplets to study individual droplet behavior; this can be done by adding PFCnDs into the phantom at step 2.4. Furthermore, since the crosslinking is due to a chemical reaction, relatively little heat is produced compared to a physical crosslinking based upon an upper critical solution temperature like gelatin. This reduces the probability for spontaneous vaporization of the embedded droplets.

While there are a variety of methods for synthesizing phantoms, polyacrylamide produces a relatively durable and non-degradable phantom that possess low acoustical attenuation[35] and optical absorption coefficient[36]. These properties can be tuned to more closely mimic the acoustic and optical properties of human tissue by adjusting the concentration of the final polyacrylamide solution and through the inclusion of particles in the phantom such as silica, glass beads, or titanium dioxide[36]. Furthermore the mechanical properties of the phantoms can be adjusted by modifying the percentage of polymer content (i.e. percentage of acrylamide and bis(acrylamide)) and percentage of crosslinker (i.e. percentage of bis(acrylamide) in total polymer content)[37]. Alternative phantoms include but are not limited to agar[38], gelatin[39], polyvinyl alcohol (PVA)[40], etc.

The critical steps for a successful imaging of activated PFCnD distribution and hyperechogenic dynamics are as follows. 1) Synchronize the laser system (activation source) and ultrasound imaging system. 2) Align the laser cross section both with target region of interest and with ultrasound imaging plane. 3) Adjust ultrasound imaging parameters proper to PFCnD imaging (i.e., framerate, pulse waveform, etc.).

The optical activation of PFCnD has a noticeable advantage over acoustically activated ones that it can evade the acoustic interference which drastically degrade the quality of ultrasound image while observing its recondensing phase in time. However, it is challenging to integrate and align the laser system with the ultrasound imaging system both spatially and temporally. The use of a 3D printed holder allows for repeatable and controlled light delivery. The light delivery can also be troubleshooted by inserting a metal rod into the inclusion in the polyacrylamide phantom as the metal rod should produce photoacoustic contrast to indicate light delivery. Temporal synchronization was achieved by building off a previously developed platform[20], which allows for both synchronization of the lasing and imaging system while keeping the full programmability of Verasonics imaging system with a user-friendly interface. Additionally, the program provides real-time conventional B-mode imaging and photoacoustic imaging to assist in troubleshooting and locating the region of interest where PFCnDs are distributed. However, this setup requires an external nanosecond pulsed laser. Currently, to our knowledge, there are a few commercial systems that have integrated laser-ultrasound imaging systems that may allow for PFCnD imaging e.g., Visualsonics (Vevo LAZR, Vevo LAZR-X, Vevo 3100, Vevo F2), Endera Nexus 128, and iTheraMedical (insight 64, inVision 128, inVision 256-TF, and inVision 512-echo).

The ultrafast ultrasound imaging of the vaporizing-recondensing behavior of PFCnD suffers mainly from low sensitivity. While most common solutions for image sensitivity enhancement

include multi-frame compounding, those techniques are limited by their inherent characteristic of degrading the framerate, since the PFCnD imaging is highly vulnerable for motion artifacts in that it includes time-differential process. The pulse polarity modulation in our protocol effectively addresses this problem in PFCnD imaging by leveraging the acoustic dynamics of vaporized PFCnDs to have more discriminable and prolonged image while not affecting temporal resolution at all.

While ODV allows for droplets with unique capabilities such as repeated vaporization and photoacoustic contrast, the activation method has limited depth penetration in comparison to ultrasound. As light penetration is limited, this restricts the applications to mainly superficial procedures such as a replacement for sentinel lymph node biopsy[41]. This limitation can potentially be bypassed through catheter based light delivery systems, allowing for activation deep in tissue. Since the contrast is acoustic, vaporization will be able to be imaged at depth comparable to ADV. An alternative activation technique may be magnetic droplet vaporization, in which magnetic contrast agents such as iron oxide nanoparticles are encapsulated within the droplet[42]. This will allow for the vaporization at any depth.

In the future, the capability of our protocol to image and modulate the hyperechogenic response of PFCnD at the same time can used to several applications where monitoring and manipulation of PFCnD are required. For example, longer detectable time can ameliorate the image quality of super-resolution imaging by giving larger number of frames to average. Furthermore, more precise control of PFCnD has potential to elevate the efficiency and safety of bubble-mediated therapeutics such as BBB opening and drug delivery.

ACKNOWLEDGMENTS:
The work was supported in part by the Breast Cancer Research Foundation under grant BCRF-20-043.

DISCLOSURES:
The authors have nothing to disclose.

REFERENCES:

1. Schutt, E. G., Klein, D. H., Mattrey, R. M., Riess, J. G. Injectable microbubbles as contrast agents for diagnostic ultrasound imaging: the key role of perfluorochemicals. *Angewandte Chemie International Edition*. **42** (28), 3218–3235 (2003).
2. Lee, H. et al. Microbubbles used for contrast enhanced ultrasound and theragnosis: a review of principles to applications. *Biomedical Engineering Letters*. **7** (2), 59–69 (2017).
3. Hobbs, S. K. et al. Regulation of transport pathways in tumor vessels: Role of tumor type and microenvironment. *Proceedings of the National Academy of Sciences*. **95** (8), 4607–4612 (1998).
4. Ishida, O., Maruyama, K., Sasaki, K., Iwatsuru, M. Size-dependent extravasation and interstitial localization of polyethyleneglycol liposomes in solid tumor-bearing mice. *International Journal of Pharmaceutics*. **190** (1), 49–56 (1999).
5. Wong, Z. Z., Kripfgans, O. D., Qamar, A., Fowlkes, J. B., Bull, J. L. Bubble evolution in acoustic

droplet vaporization at physiological temperature via ultra-high speed imaging. *Soft Matter*. **7** (8), 4009 (2011).
6. Yu, J., Chen, X., Villanueva, F. S., Kim, K. Vaporization and recondensation dynamics of indocyanine green-loaded perfluoropentane droplets irradiated by a short pulse laser. *Applied Physics Letters*. **109** (24), 243701 (2016).
7. Kripfgans, O. D., Fowlkes, J. B., Miller, D. L., Eldevik, O. P., Carson, P. L. Acoustic droplet vaporization for therapeutic and diagnostic applications. *Ultrasound in Medicine & Biology*. **26** (7), 1177–1189 (2000).
8. Aliabouzar, M., Kumar, K. N., Sarkar, K. Acoustic vaporization threshold of lipid-coated perfluoropentane droplets. *The Journal of the Acoustical Society of America*. **143** (4), 2001–2012 (2018).
9. Sheeran, P. S., Luois, S., Dayton, P. A., Matsunaga, T. O. Formulation and acoustic studies of a new phase-shift agent for diagnostic and therapeutic ultrasound. *Langmuir*. **27** (17), 10412–10420 (2011).
10. Sheeran, P. S., Luois, S. H., Mullin, L. B., Matsunaga, T. O., Dayton, P. A. Design of ultrasonically-activatable nanoparticles using low boiling point perfluorocarbons. *Biomaterials*. **33** (11), 3262–3269 (2012).
11. Wilson, K., Homan, K., Emelianov, S. Biomedical photoacoustics beyond thermal expansion using triggered nanodroplet vaporization for contrast-enhanced imaging. *Nature Communications*. **3** (1), 618 (2012).
12. Strohm, E., Rui, M., Gorelikov, I., Matsuura, N., Kolios, M. Vaporization of perfluorocarbon droplets using optical irradiation. *Biomedical Optics Express*. **2** (6), 1432 (2011).
13. Wei, C. et al. Laser-induced cavitation in nanoemulsion with gold nanospheres for blood clot disruption: in vitro results. *Optics Letters*. **39** (9), 2599 (2014).
14. Hannah, A., Luke, G., Wilson, K., Homan, K., Emelianov, S. Indocyanine green-loaded photoacoustic nanodroplets: Dual contrast nanoconstructs for enhanced photoacoustic and ultrasound imaging. *ACS Nano*. **8** (1), 250–259 (2014).
15. Lajoinie, G. et al. Ultrafast vapourization dynamics of laser-activated polymeric microcapsules. *Nature Communications*. **5** (1), 3671 (2014).
16. Hannah, A. S., Luke, G. P., Emelianov, S. Y. Blinking phase-change nanocapsules enable background-free ultrasound imaging. *Theranostics*. **6** (11), 1866–1876 (2016).
17. Santiesteban, D. Y., Hallam, K. A., Yarmoska, S. K., Emelianov, S. Y. Color-coded perfluorocarbon nanodroplets for multiplexed ultrasound and photoacoustic imaging. *Nano Research*. **12** (4), 741–747 (2019).
18. Luke, G. P., Hannah, A. S., Emelianov, S. Y. Super-resolution ultrasound imaging in vivo with transient laser-activated nanodroplets. *Nano Letters*. **16** (4), 2556–2559 (2016).
19. Zhu, Y. I., Yoon, H., Zhao, A. X., Emelianov, S. Y. Leveraging the imaging transmit pulse to manipulate phase-change nanodroplets for contrast-enhanced ultrasound. *IEEE Transactions on Ultrasonics, Ferroelectrics, and Frequency Control*. **66** (4), 692–700 (2019).
20. Yoon, H., Zhu, Y. I., Yarmoska, S. K., Emelianov, S. Y. Design and demonstration of a configurable imaging platform for combined laser, ultrasound, and elasticity imaging. *IEEE Transactions on Medical Imaging*. **38** (7), 1622–1632 (2019).
21. Taylor, P. Ostwald ripening in emulsions. *Advances in Colloid and Interface Science*. **75** (2), 107–163 (1998).

22. Freire, M. G., Dias, A. M. A., Coelho, M. A. Z., Coutinho, J. A. P., Marrucho, I. M. Aging mechanisms of perfluorocarbon emulsions using image analysis. *Journal of Colloid and Interface Science*. **286** (1), 224–232 (2005).
23. Yarmoska, S. K., Yoon, H., Emelianov, S. Y. Lipid shell composition plays a critical role in the stable size reduction of perfluorocarbon nanodroplets. *Ultrasound in Medicine & Biology*. **45** (6), 1489–1499 (2019).
24. Sheeran, P. S. et al. Decafluorobutane as a phase-change contrast agent for low-energy extravascular ultrasonic imaging. *Ultrasound in Medicine & Biology*. **37** (9), 1518–1530 (2011).
25. Lin, S. et al. Optically and acoustically triggerable sub-micron phase-change contrast agents for enhanced photoacoustic and ultrasound imaging. *Photoacoustics*. **6**, 26–36 (2017).
26. Sheeran, P. S. et al. Methods of generating submicrometer phase-shift perfluorocarbon droplets for applications in medical ultrasonography. *IEEE Transactions on Ultrasonics, Ferroelectrics, and Frequency Control*. **64** (1), 252–263 (2017).
27. Shui, L., van den Berg, A., Eijkel, J. C. T. Scalable attoliter monodisperse droplet formation using multiphase nano-microfluidics. *Microfluidics and Nanofluidics*. **11** (1), 87–92 (2011).
28. Jeong, W.-C. et al. Controlled generation of submicron emulsion droplets via highly stable tip-streaming mode in microfluidic devices. *Lab on a Chip*. **12** (8), 1446 (2012).
29. Xu, X. et al. Microfluidic production of nanoscale perfluorocarbon droplets as liquid contrast agents for ultrasound imaging. *Lab on a Chip*. **17** (20), 3504–3513 (2017).
30. Song, R., Peng, C., Xu, X., Zou, R., Yao, S. Facile fabrication of uniform nanoscale perfluorocarbon droplets as ultrasound contrast agents. *Microfluidics and Nanofluidics*. **23** (1), 12 (2019).
31. Liedtke, S., Wissing, S., Müller, R. H., Mäder, K. Influence of high-pressure homogenisation equipment on nanodispersions characteristics. *International Journal of Pharmaceutics*. **196** (2), 183–185 (2000).
32. Reznik, N., Williams, R., Burns, P. N. Investigation of vaporized submicron perfluorocarbon droplets as an ultrasound contrast agent. *Ultrasound in Medicine & Biology*. **37** (8), 1271–1279 (2011).
33. Grapentin, C., Barnert, S., Schubert, R. Monitoring the stability of perfluorocarbon nanoemulsions by cryo-TEM image analysis and dynamic light scattering. *Plos One*. **10** (6), e0130674 (2015).
34. de Gracia Lux, C. et al. Novel method for the formation of monodisperse superheated perfluorocarbon nanodroplets as activatable ultrasound contrast agents. *RSC Advances.* **7** (77), 48561–48568 (2017).
35. Zell, K., Sperl, J. I., Vogel, M. W., Niessner, R., Haisch, C. Acoustical properties of selected tissue phantom materials for ultrasound imaging. *Physics in Medicine and Biology*. **52** (20), N475–N484 (2007).
36. Hariri, A. et al. Polyacrylamide hydrogel phantoms for performance evaluation of multispectral photoacoustic imaging systems. *Photoacoustics*. **22**, 100245 (2021).
37. Denisin, A. K., Pruitt, B. L. Tuning the range of polyacrylamide gel stiffness for mechanobiology applications. *ACS Applied Materials & Interfaces*. **8** (34), 21893–21902 (2016).
38. Rajagopal, S., Sadhoo, N., Zeqiri, B. Reference characterisation of sound speed and attenuation of the iec agar-based tissue-mimicking material up to a frequency of 60 MHz. *Ultrasound in Medicine & Biology*. **41** (1), 317–333 (2015).

39. Madsen, E. L., Zagzebski, J. A., Banjavie, R. A., Jutila, R. E. Tissue mimicking materials for ultrasound phantoms. *Medical Physics*. **5** (5), 391–394 (1978).
40. Kharine, A. et al. Poly(vinyl alcohol) gels for use as tissue phantoms in photoacoustic mammography. *Physics in Medicine and Biology*. **48** (3), 357–370 (2003).
41. Kim, H., Chang, J. H. Multimodal photoacoustic imaging as a tool for sentinel lymph node identification and biopsy guidance. *Biomedical Engineering Letters*. **8** (2), 183–191 (2018).
42. Zhou, Y. et al. Magnetic nanoparticle-promoted droplet vaporization for in vivo stimuli-responsive cancer theranostics. *NPG Asia Materials*. **8** (9), e313–e313 (2016).

Figure1

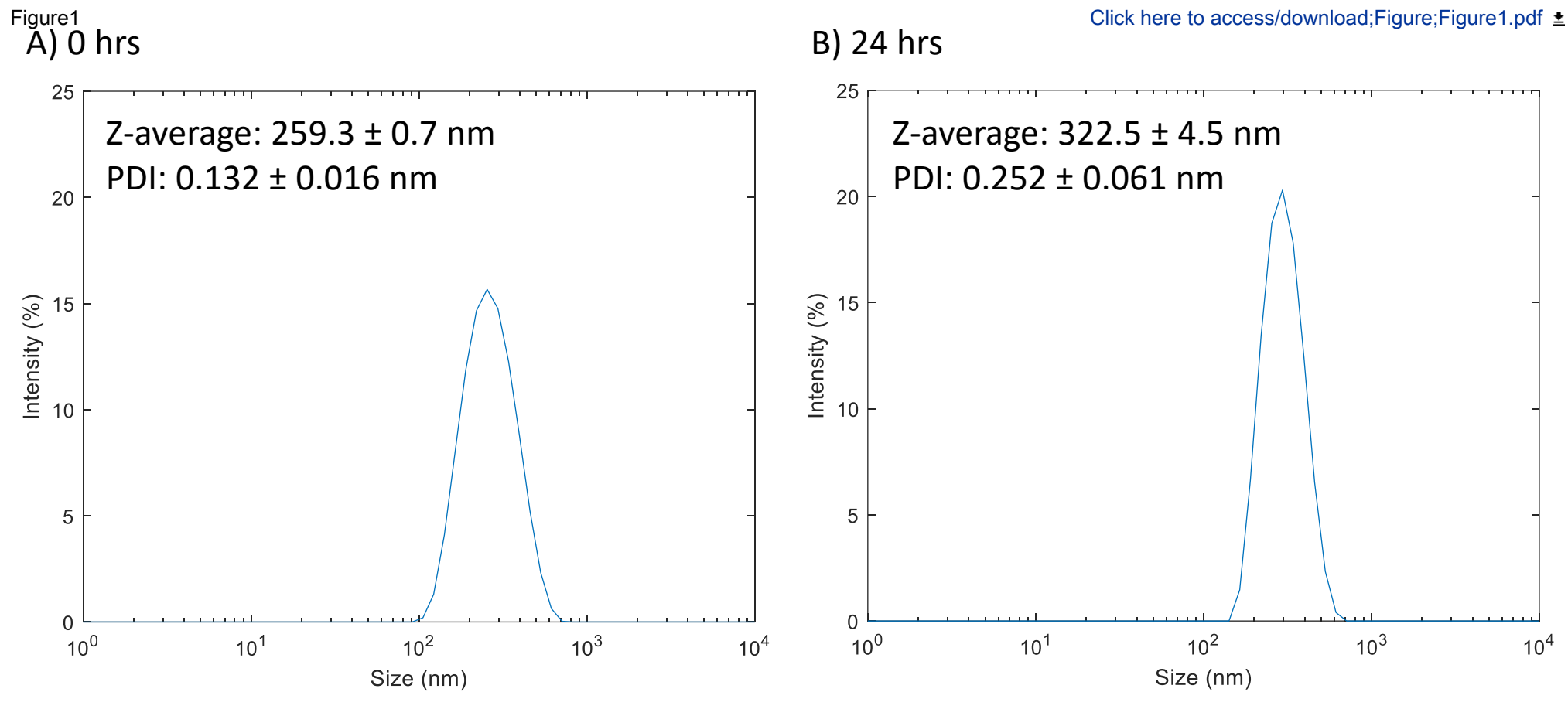

Figure2

A)

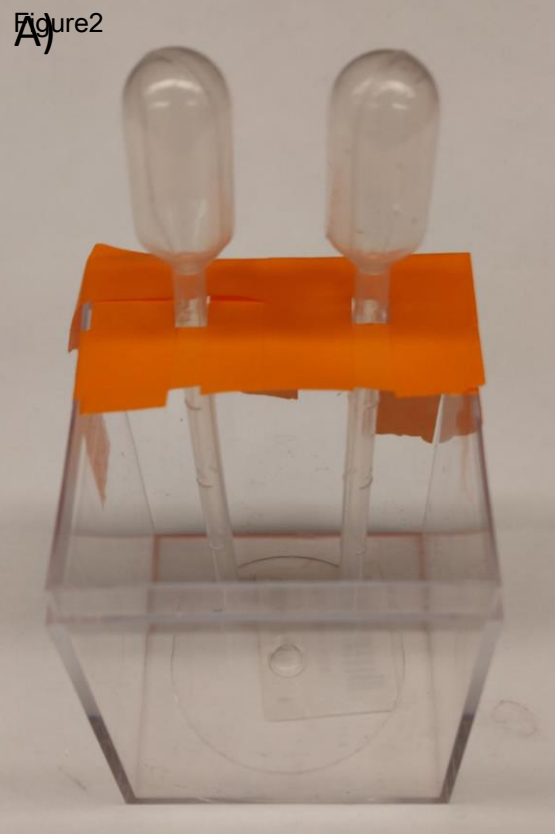

B)

Click here to access/download;Figure;Figure2.pdf

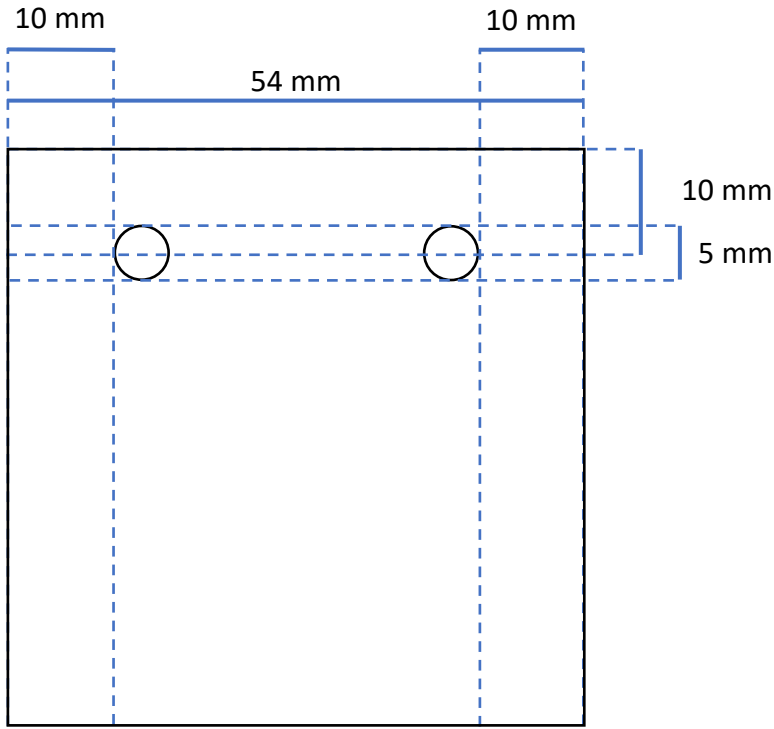

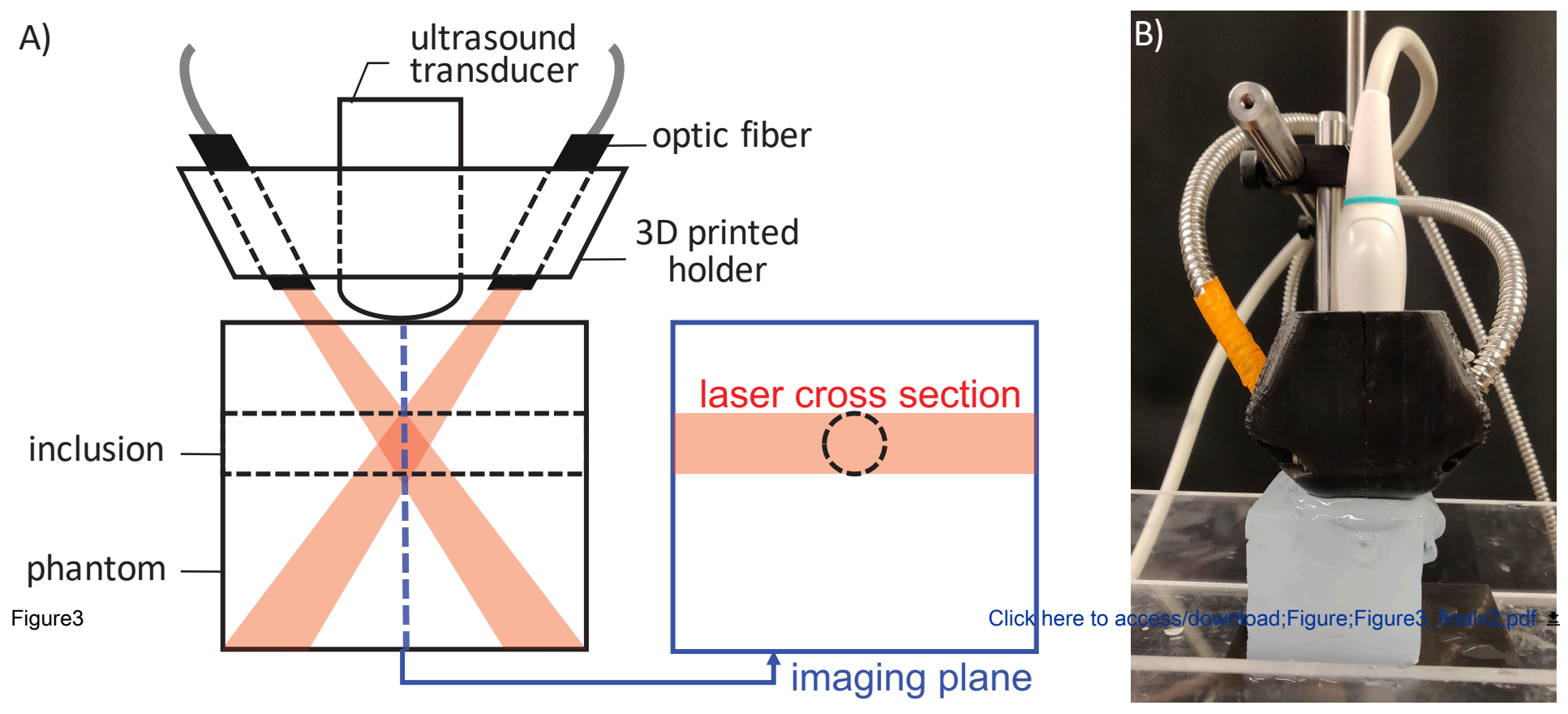

Figure3

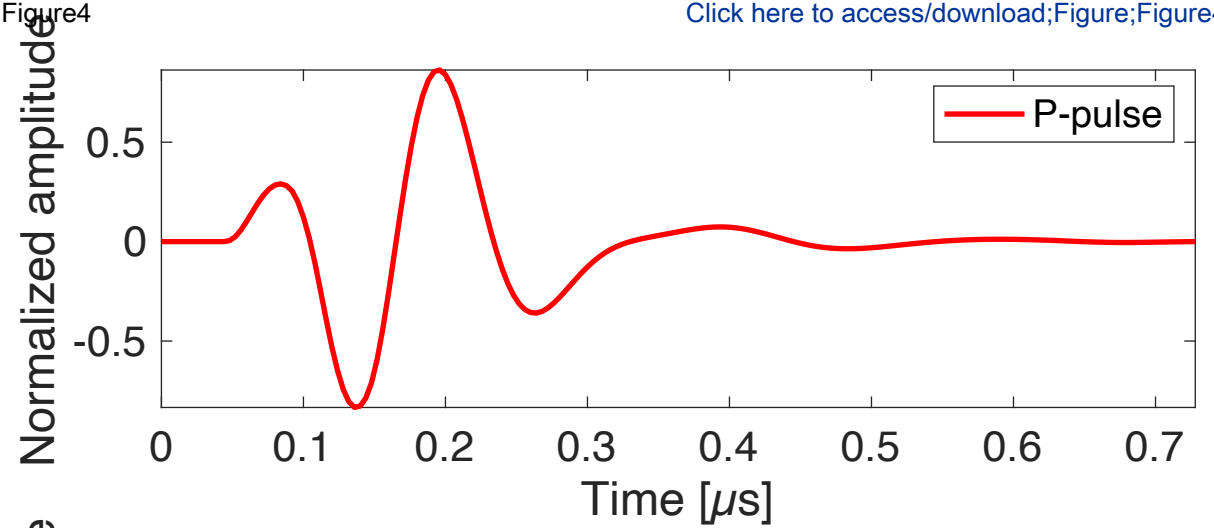

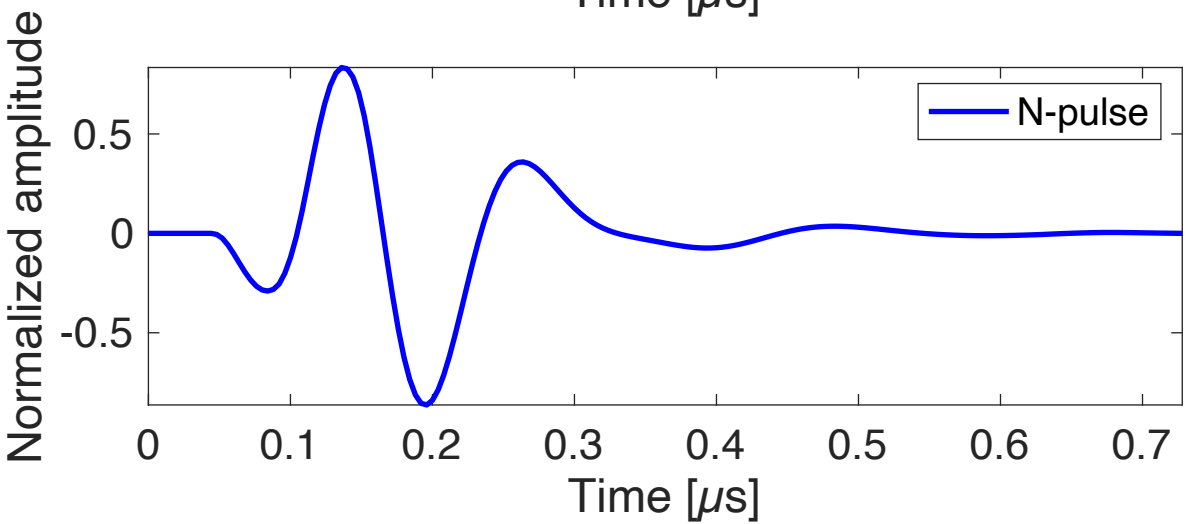

Figure5

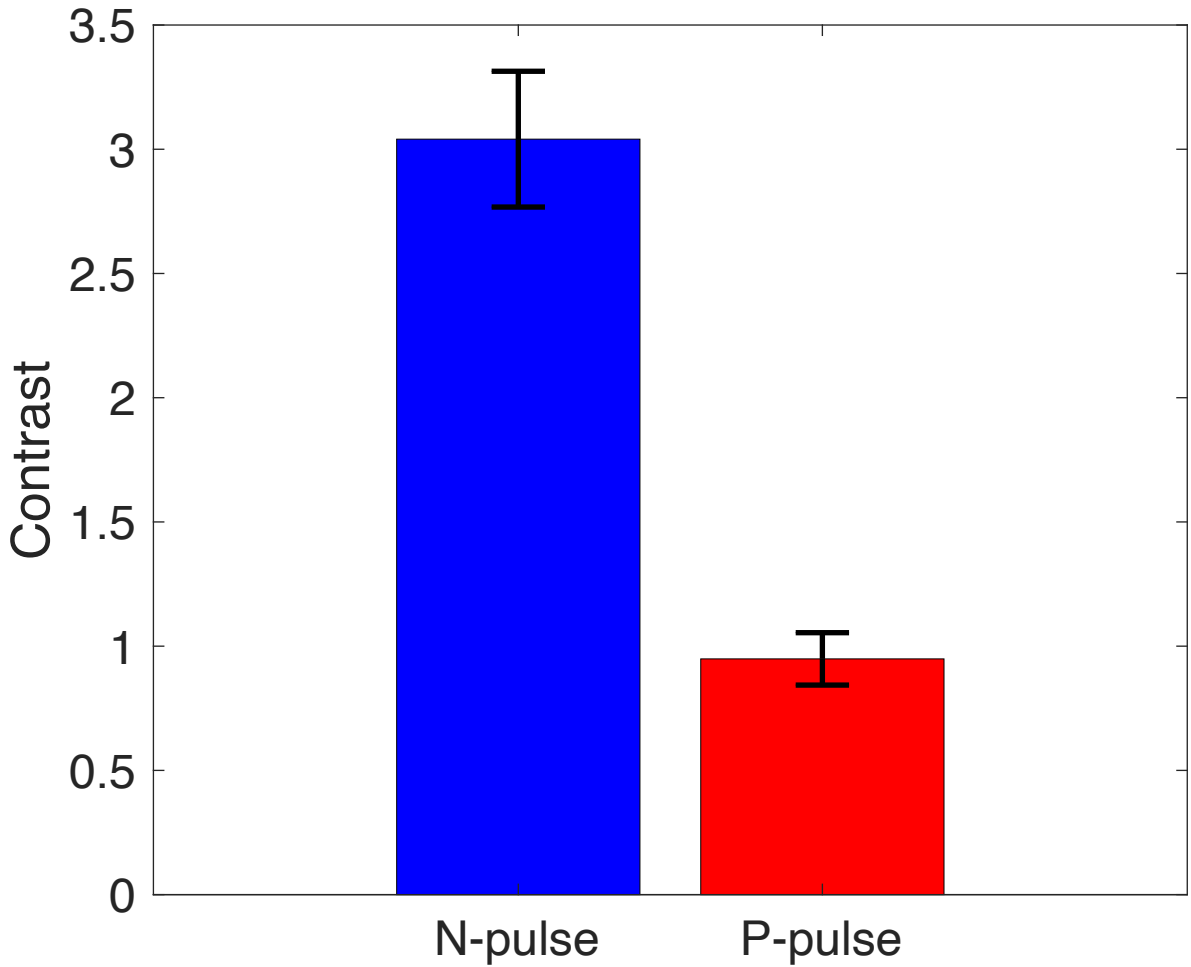

Figure6

Click here to access/download;Figure;Figure6.pdf

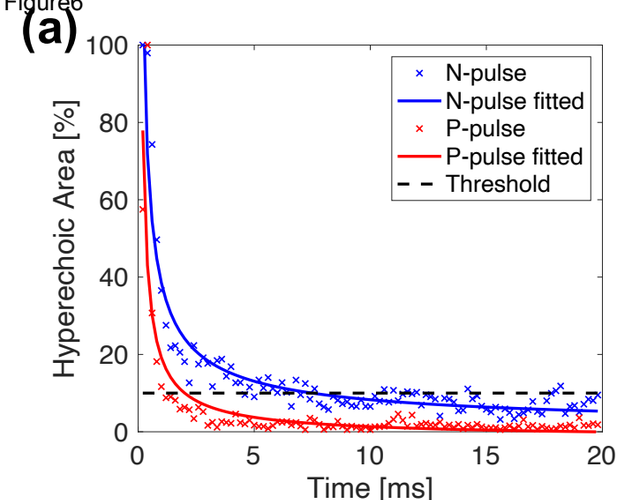

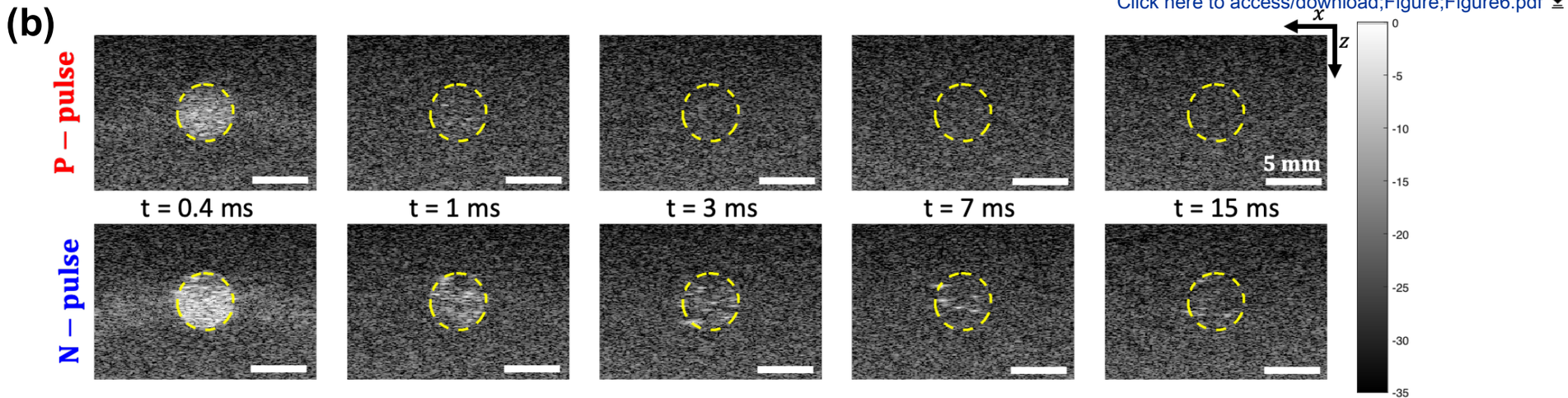

Table

Total Volume of Phantom (mL)	50	100	250	500
DI water (mL)	37.5	74.9	187.4	375
40% PA solution (mL)	12.5	25.1	62.6	125
Silica (mg)	100	200	500	1000
10% APS solution (µL)	500	1000	2500	5000
TEMED (µL)	62.5	125	312.5	625

Table of Materials

Click here to access/download

Table of Materials

JoVE_MaterialsRevised.xls

Formulation and Acoustic Modulation of Optically Vaporized Perfluorocarbon Nanodroplets

Andrew Zhao, Jeungyoon Lee, Stanislav Emelianov

We appreciate the input and constructive comments given by the reviewers and have revised our manuscript accordingly, leading to an improved and hopefully acceptable paper for publication in JOVE. Below please find the specific text sections that required revisions, split into three sections: response to editors and the two reviewers. In each section we list the editor/reviewer comments, followed by our responses. As there have been numerous changes, only specific changes outside of the protocol have been highlighted. The rest of the changes have been tracked through Microsoft word's native "Track Changes" function.

Response to Editorial comments

"1. Please take this opportunity to thoroughly proofread the manuscript to ensure that there are no spelling or grammar issues. Please define all abbreviations at first use.
2. Please increase the word count of the abstract to be 150-300 words.
3. For in-text formatting, corresponding reference numbers should appear as numbered superscripts after the appropriate statement(s) but BEFORE punctuation.
4. Please revise the text, especially in the protocol, to avoid the use of any personal pronouns (e.g., "we", "you", "our" etc.).
5. Please ensure that all text in the protocol section is written in the imperative tense as if telling someone how to do the technique (e.g., "Do this," "Ensure that," etc.). The actions should be described in the imperative tense in complete sentences wherever possible. Avoid usage of phrases such as "could be," "should be," and "would be" throughout the Protocol. Any text that cannot be written in the imperative tense may be added as a "Note." However, notes should be concise and used sparingly. Please include all safety procedures and use of hoods, etc."

We appreciate the guidance and have made changes to conform with the requirements. They are too numerous to list individually here, but changes have been tracked in the word document.

"6. Please note that your protocol will be used to generate the script for the video and must contain everything that you would like shown in the video. Please add more details to your protocol steps. Please ensure you answer the "how" question, i.e., how is the step performed? Alternatively, add references to published material specifying how to perform the protocol action. There should be enough detail in each step to supplement the actions seen in the video so that viewers can easily replicate the protocol."

The protocol has been expanded to include more details along with pictures of certain setups and pictures of mold preparation (Fig 2) to allow for easier replication. We have altered the text substantially to include more descriptions of how to perform the procedure.

"7. I) 2.1.1: How much water should be added to the vacuum flask?
ii) 2.3: How much 10% acrylamide-bisacrylamide solution should be prepared in the beaker?
iii) 2.4: solution from step 2.3?
iv) 2.5: How do you prepare the mold—with what?"

These details have been included in the protocol. Specifically, 400 mL of DI water in the vacuum flask and a 200 mL solution of 10% acrylamide-bisacrylamide solution. In step 2.4, silica was added to the solution in step 2.3, and a better description of step 2.5 was added along with an image of how the mold should be prepared (Figure 2).

"8. Please highlight up to 3 pages of the Protocol (including headings and spacing) that identifies the essential steps of the protocol for the video, i.e., the steps that should be visualized to tell the most cohesive story of the Protocol. This will ensure that filming will be completed in one day. Remember that non-highlighted Protocol steps will remain in the manuscript, and therefore will still be available to the reader."

A section of the protocol has been highlighted in yellow.

"9. Please include a scale bar for all images taken with a microscope to provide context to the magnification used. Define the scale in the appropriate Figure Legend."

We assumed that the editor was referring to the ultrasound images in what is now figure 6. Scale bars were added to all images in the set and defined in the figure legend.

"10. Include at least 10 references."

References were added as the background and discussion were expanded.

Response to Reviewer 1:

"There are many experimental description flaws and missing details. The main weaknesses are that the level of clarity and experimental details are higher in the original description of the work (current ref 9)."

We appreciate the reviewer's feedback and have made several changes to the manuscript to enhance the clarity and experimental details. The protocol section for both the formulation and imaging has been completely rewritten.

"Another important point that justifies the need of editing is the absence of key references but a too important numbers of self citations (5 out of 9 total references)."

We have expanded the discussion and introduction with proper sources. While there are still a significant number of self citations (8 out of 42), we are the only group working on this particular formulation of optical droplets and our work builds upon our previous publications, necessitating the need to cite them to justify certain claims about their performance/capabilities and software developed to image them.

"Finally, the manuscript is very short and only provides a vague overview. All the sections of the paper need to be expanded. It would be useful to include figures of the actual set up and not only schemes. "

We have expanded most sections and rewritten the discussion, methods, and representative results within the manuscript to fall in line with JOVE's requirements and included pictures of the set-ups to go along with the schemes (Figures 2 and 3).

"An overview of the advantages and limitations (including the efficacy in deep tissue) for potential clinical applications could be discussed."

We have included a brief discussion about the advantages and limitations of utilizing ODV for clinical applications along with some potential methods of bypassing some of these limitations. This has been highlighted in red.

"Abstract and elsewhere. The word "synthesis" is not appropriate here but should be changed for "Formulation"… Representative results. "synthesis and synthesized emulsion" should be replaced by "formulation and obtained nanoparticles" or something similar."

We appreciate and agree with the suggestion. The phrasing has been changed as recommended.

"Protocol. The authors should specify the precautions to follow when using IR dyes (temperature, light….). The authors should report both temperature and sonication time."

We have included additional instructions on the covering of the samples in aluminum foil or performing certain steps in dim conditions to prevent photobleaching. Sonication steps have been modified to include both time and temperature as needed. All sonication was performed at room temperature and the manuscript has been updated accordingly.

"" Perfluorohexane exhibits a degree of volatility that may cause it to leak out of the pipette". Density is rather the issue here as perfluorohexane will most likely not evaporate during the few seconds it takes to transfer it. Due to its higher density than water, pipettes are not designed to

accurately measure liquid perfluorocarbon. Alternatively, weighting the required amount will be the most accurate choice."

We appreciate the additional insight on the difficulties of handling perfluorohexane with air-displacement pipettes. However, perfluorohexane is volatile. It possess a similar boiling point and partial pressure as acetone, and leakage will result in a noticeable error especially when dealing with volumes of 50µL. Furthermore, due to its volatility, accurately weighing the pipetted volume (50µL) will be difficult, as the mass will have changed in the time it takes for the balance to achieve equilibrium. We have included this information within the discussion section (highlighted in light blue), with the strong recommendation to use a positive-displacement pipette.

"Step 1.8 is missing some characterization including concentration, and some stability data...

Z average and PDI should be reported."

We have included the PDI/Z average for the DLS data and concentration measurements from a nanosight NS300, along with 24 hour stability measurements (Figure 1 A and B).

"Step 2.1: "de-gas" should be replaced by "degassed". Step 2.11 is useless and should be placed under step 2.1. Steps 2.5 is not clearly explained and would benefit from a figure."

We appreciate the feedback and have been updated typo in the protocol accordingly. A picture of the prepared mold has been provided for step 2.5 (Figure 2).

"Discussion. Previously published protocols/papers are not cited properly as there are no references cited in the entire discussion section. "produces a large number of droplets". The authors should provide actual measured concentrations. In addition, high-pressure homogenization should also be mentioned (with refs) as a technique of choice to generate monodisperse and high nanoparticle counts."

We have substantially rewritten the discussion to include comparisons to other methods including high-pressure homogenization along with appropriate citations. The main changes are highlighted in dark blue. In addition, an approximate concentration is provided based on measurements from a nanosight NS300.

Response to Reviewer 2:

"The authors should clearly define "nanoparticles extravasation" and the requirements in terms of size depending on the intended clinical indication/use"

We have included a bit more discussion about extravasation, however, a detailed description of the size for different clinical uses is outside the scope of the original manuscript and may have limited benefit, as each cited value may be only applicable for specific animal models/disease states within a certain animal model. Furthermore there is even debate as to the importance of size for extravasation[1, 2]. The changes made are highlighted in dark green.

"The authors indicate five-fold increase in diameter upon ODV phenomenon. To support that statement, please provide data or relevant references using similar formulation composition and ODV settings."

We have updated the claim with references to somewhat similar droplets and made modification to agree with some observations in the literature. Due to the nature of visualizing the vaporization, the droplets used for these experiments are on the scale of micrometers as high speed cameras are unable to visualize vaporization of nanoscale nanodroplets. Additionally it is unclear how much impact the surfactant shell has upon the increase in diameter as most results suggest a ~4-5 fold increase for low boiling point perfluorocarbon cores. It is unclear how this would change for higher boiling points, but work by Yu et. al[3] suggests that recondensable droplets may not expand to the same degree. The change is highlighted in green.

"As described by the authors, the shell composition is made of DSPC and DSPE-PEG2000, while IR1048 is added as an optical absorber. However, based on the authors description (See Lines 82-84); this make a formulation mainly composed of DSPE-PEG2000 (52.8% molar ratio), very low DSPC ratio (7.5%) and an excess amount of fluorophore dye (~40% molar ratio). Could you please double check the amount of the different ingredients?"

We appreciate the reviewer's attention to detail. The formulation is correct. The inverse ratio is based upon work done previous in our lab, where this ratio was found to produce smaller and more consistently sized droplets[4].

"In the last part of nanodroplets synthesis, is there any risk to breakdown the nandroplets while sonicating in a bath sonicator for 1 min?"

This is a good point. It is possible that sonication would result in droplet breakdown, however results from a previous paper from our group suggests its mainly the larger droplets that do end up breaking down as the size distribution narrows after prolonged sonication[4].

"The authors are indicating a size range of PFCnD around 200-300 nm without any data regarding the polydispersity. This can be measured using the zeta sizer nanoZS. In addition, it is stated that

the method is relatively rapid and produces many droplets compared to other procedures including microfluidic technology. However, data concerning the PFCnD concentration is missing!"

This information has been added in the manuscript in Figure 1 and concentration data taken from the nanosight NS300 has been included in the manuscript.

"The use of tissue mimicking phantoms (TMPs) is of utmost importance to reduce preclinical in vivo requirements for clinical translation. Materials such as agar, gelatin, or polyacrylamide have been reported (See references below).
* C. Lafon et al. Ultrasound in Med. & Biol., Vol. 31, No. 10, pp. 1383-1389, 2005
* M. Zhang et al. Acad Radiol. 2011; 18(9): 1123-1132
* A. Eranki et al. International Journal of Hyperthermia 2019, VOL. 36, NO. 1, 517-528"

We have included a brief mention of different TMPs for US imaging with relevant citations (highlighted in pink).

"Did the authors characterize the polyacrylamide material to make sure it is comparable to human soft tissues in terms of physical, thermal, and acoustic properties?"

We have not characterized these properties as many of them require specialized equipment to make accurate measurements. However, the polyacrylamide phantoms are based upon published protocols that have been characterized and citations for those papers have been added to the manuscript and a brief discussion on methods of tuning these properties has been added (highlighted in pink).

"What about further clinical translation of the approach? Is there any commercially available device combing both laser acting as activation system and ultrasound imaging system? As raised by the authors, the spatiotemporal alignment is rather challenging."

One potential clinical translation of the approach is for supplanting sentinel lymph node biopsy. The sentinel lymph node is generally superficial and contrast agents that drain from the tumor to that node theoretically can be detected. Some commercially available laser and ultrasound imaging system include the instruments from Visualsonics (Vevo LAZR, VEVO LAZRX, VEVO 3100, VEVO F2), Endera Nexus 128 and iTheraMeidcal (insight 64, inVision 128, inVision 256-TF, and inVision 512-echo). The vantage research ultrasound system can be interfaced with an external pulsed laser to allow for programmable triggering and photoacoustic imaging. A brief mention of alternative systems has been added and highlighted in grey.

"Finally, how to deal with the shallow penetration depth of the laser system which might limit the system application to selected clinical indications?"

The shallow depth penetration is a major limitation for photoacoustic imaging in general. Even utilizing the second optical window, depth penetration is generally limited to ~1 cm. However, as the contrast generated from photoacoustics is acoustic in nature, if the contrast agents are triggered at depth, contrast can still be identified. As such a catheter based light delivery system can be utilized to activate droplets at depths in a way that is minimally invasive.

"In the table of materials, the catalog number "90-1083C?" of the laser system needs to be clarified."

We appreciate the reviewer's attention to detail. The catalog number for the laser system has been removed as we mistook the quote number for the catalog number. The system itself does not have a catalog number.

References:

1. Smith, B.R. *et al.* Shape Matters: Intravital Microscopy Reveals Surprising Geometrical Dependence for Nanoparticles in Tumor Models of Extravasation. *Nano Letters*. **12** (7), 3369–3377, doi: 10.1021/nl204175t (2012).
2. Moghimi, S.M., Simberg, D. Nanoparticle transport pathways into tumors. *Journal of Nanoparticle Research*. **20** (6), 169, doi: 10.1007/s11051-018-4273-8 (2018).
3. Yu, J., Chen, X., Villanueva, F.S., Kim, K. Vaporization and recondensation dynamics of indocyanine green-loaded perfluoropentane droplets irradiated by a short pulse laser. *Applied Physics Letters*. **109** (24), 243701, doi: 10.1063/1.4972184 (2016).
4. Yarmoska, S.K., Yoon, H., Emelianov, S.Y. Lipid Shell Composition Plays a Critical Role in the Stable Size Reduction of Perfluorocarbon Nanodroplets. *Ultrasound in Medicine & Biology*. **45** (6), 1489–1499, doi: 10.1016/j.ultrasmedbio.2019.02.009 (2019).